

## Molecular-dynamics simulation of the energetic deposition of Ag thin films

C. M. Gilmore\* and J. A. Sprague

*Surface Modification Branch, U.S. Naval Research Laboratory, Washington, D.C. 20375*

(Received 8 April 1991)

A three-dimensional molecular-dynamics simulation of the growth of 500 energetic Ag atoms incident on a substrate with 1008 Ag atoms was conducted with the atomic interactions modeled by the embedded-atom method. The substrate temperature was 300 K and incident-Ag-atom energies ranged from 0.1 to 10 eV. For all incident-atom energies the growth was epitaxial. For low incident-atom energies the surface topography was three-dimensional islands, but the growth changed progressively towards layer-by-layer (Frank-van der Merwe) growth as the incident-atom energy increased to 10 eV. At low incident-atom energy (0.1 eV) the primary mechanism for redistribution of atoms between layers of the film was the collapse of unstable configurations of atoms. For higher incident-atom energies (1.0 and 10.0 eV) the primary redistribution mechanism was ballistic displacement. At low fractional layer coverage, both perfect-crystal and stacking-fault sites were occupied; for larger layer coverage, however, all of the atoms in a single layer tended to occupy one type of site, although both perfect and stacking-fault layers were observed.

### INTRODUCTION

The deposition of thin films with energetic atoms is of interest because of the observation that the character of a thin film can be altered by utilizing energetic atoms during the deposition process. Some of the characteristics that can be varied include crystal orientation,<sup>1</sup> chemistry,<sup>2</sup> density, and microstructure.<sup>3</sup> Several authors have observed that epitaxial thin films can be grown at lower temperatures if atoms of a few electron volts energy are utilized rather than atoms with only thermal energy, as from a molecular-beam deposition system.<sup>4,5</sup>

This research program was directed at understanding the mechanisms that result in microstructure changes during energetic-atom deposition, and more specifically to determine how energetic atoms affect epitaxial crystal growth. Brice, Tsao, and Picraux have utilized Monte Carlo calculations to study the displacements of surface and bulk atoms by energetic incident ions. They concluded that molecular-dynamics simulations are needed for the energies less than 100 eV in order to examine more accurately the energy regime where the threshold for surface-atom displacements occurs. Since the only currently available computer simulation technique that can follow the detailed motion of low-energy incident atoms during the growth of a thin film is a molecular-dynamics simulation (MDS), this is the only simulation technique that will be considered in this introduction. Also only papers that emphasize the effects of energetic atoms will be considered.

Henderson and co-workers conducted a MDS of normal thermal deposition with a hard ball potential where the atoms were allowed to relax to the nearest minimum-energy position. They observed that a porous columnar structure was formed.<sup>7</sup> Gilmer and co-workers obtained similar results from a three-dimensional model that utilized a Lennard-Jones (LJ) pair potential in conjunction

with a MDS that followed each atom until it decayed in energy to 0.01% of its initial value, after which the atom was regarded as deposited and not moved further. Several beam temperatures were utilized including  $\frac{2}{7}T_m$  and  $\frac{20}{7}T_m$ , where  $T_m$  is the LJ melting point. Films deposited at  $\frac{2}{7}T_m$  were less dense than those deposited at  $\frac{20}{7}T_m$ , the former films being very porous. The  $\frac{2}{7}T_m$  atoms moved approximately 1 atom diameter following impact, whereas the  $\frac{20}{7}T_m$  atoms moved approximately 4 atom diameters. Greater crystalline order was observed in the  $\frac{20}{7}T_m$  films, although this was not quantitatively reported.

Schneider, Rahman, and Schuller<sup>9</sup> studied the vapor deposition of LJ atoms with a three-dimensional molecular-dynamics simulation. They utilized a source temperature of approximately  $1.3T_m$  and reported results for substrate temperatures of 0 and  $0.57T_m$ . They reported that the growth was into well-ordered layers for all substrate temperatures, meaning that the atoms were located in fcc positions, but that the films grew with the layers close to the substrate having the greatest number of atoms and layers further away from the substrate having fewer atoms. The vacancy clusters in the layers close to the substrate were eventually filled with high-mobility atoms, eventually completely filling these layers. The authors reported that they expected incomplete filling of the lower layers at lower substrate temperatures, but this was not demonstrated. The research discussed above was for a MDS of thin-film growth where the source energy was thermal; the following will review a MDS of thin-film growth with more energetic sources.

Müller conducted a two-dimensional MDS with LJ atoms similar to Ni; Ni-vapor atoms arrived at the substrate with an energy of 0.1 eV. In addition, Ar atoms with kinetic energies between 10 and 100 eV were incident upon the Ni substrate.<sup>10</sup> The Ar ions were as-

sumed to interact with the substrate through a Molière potential and the attractive components of the Ar-Ar and Ar-Ni interactions were neglected. Müller found that energetic Ar ions increased the packing density and the degree of Ni homoepitaxy. This effect increased with increasing Ar-ion energy from 10 to 50 eV. These effects were primarily attributed to a forward-sputtering mechanism, where atoms overhanging a void region were forward sputtered into the void. This mechanism prevented voids from being closed over. In addition, energetic ions were observed to cause significant surface-atom displacements that tended to close up voids. Müller has also reported a similar study utilizing only LJ interactions, and similar results were obtained.<sup>11</sup>

Dodson and co-workers investigated low-energy (10–100 eV) atom-beam deposition of Si modeled with a Dodson potential utilizing MDS.<sup>12–14</sup> The substrate sizes were 96 and 384 atoms, the substrate surface was the (111) orientation, and 30 atoms were utilized to form the films. For the 10-eV atoms with normal incidence, it was found that about 30% of the atoms came to rest on the surface and 70% came to rest at interstitial sites in the first atomic double layer. No surface sputtering was observed for this energy.

To date no authors have reported on a full three-dimensional simulation of energetic-atom thin-film growth with a sufficient number of film atoms to observe film formation. Müller's simulation was two-dimensional (2D),<sup>10,11</sup> while Dodson and co-workers' results were for only 30 atoms, and mainly the trajectories and final locations of individual atoms were reported.

In this work a full three-dimensional MDS of energetic-atom thin-film growth was conducted with 500 Ag atoms deposited onto a substrate of 1008 Ag atoms. Incident atom energies from 0.1 to 10 eV were utilized.

## COMPUTER SIMULATION

The Ag-Ag interactions were all simulated with the embedded-atom method (EAM),<sup>15</sup> using the Ag potentials of Foiles, Baskes, and Daw.<sup>16</sup> The EAM has been shown to be quite effective at modeling surface properties.<sup>17</sup> This is probably due to the local electron density that is calculated at the surface and the many-body effects that are introduced through the embedding energy.

The substrate contained 1008 atoms with the (111) planes normal to the substrate surface, forming six layers of (111) planes containing 168 atoms each. This thickness was sufficient that atoms from the bottom layer of the substrate were not ejected as a result of impact by 10-eV incident atoms, although some roughening of the bottom substrate layer was observed for this impact energy, as will be discussed with the results. The substrate dimensions were  $14.1 \times 34.8 \times 35.1 \text{ \AA}^3$ , as shown in Fig. 1 where the  $x$  direction is normal to the substrate; and periodic boundary conditions were utilized in the  $Y$  and  $Z$  directions. To keep the entire substrate from moving as a result of impact of the energetic atoms, three atoms in the plane farthest from the surface had their velocities set to zero throughout the simulation. This fixed the location of the substrate in space. The three atoms chosen for fixing were the ones with the largest velocities after an initial equilibration time of 5 ps. These atoms should have been close to their equilibrium positions. Other than the constraint of these three atoms and the application of periodic boundary conditions, the positions of all other atoms were determined with the equations of motion that were integrated with the Nordsieck technique.<sup>18</sup> The dynamic code 5.2 of Daw and Foiles was utilized for the molecular-dynamics simulation.<sup>19</sup>

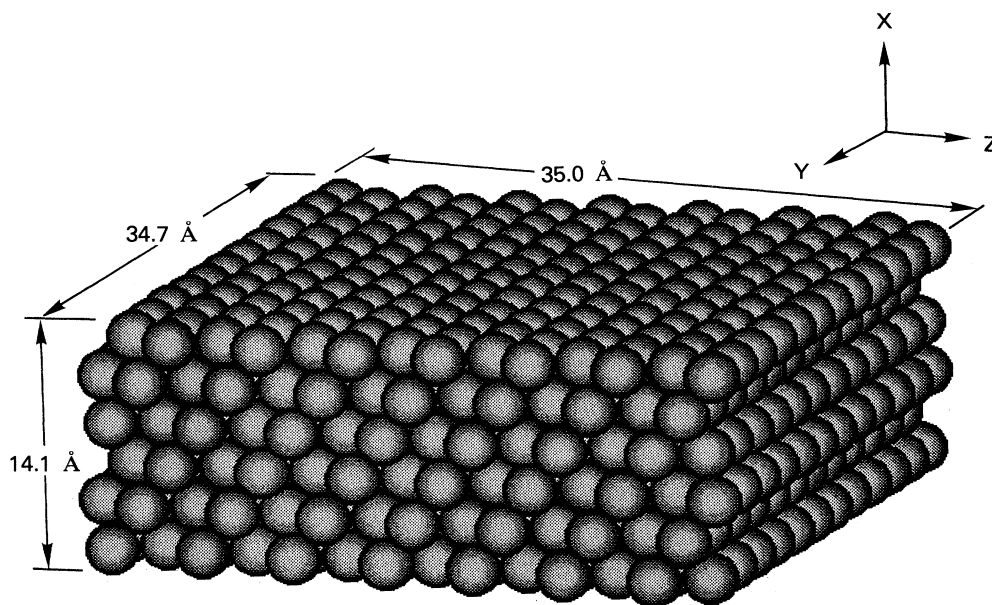


FIG. 1. Simulation configuration showing the substrate atoms and dimensions. Atoms were incident in the  $-X$  direction.

The energetic vapor-phase atoms were started at a distance from the growing thin film that was sufficiently large that the incident atom did not initially interact with the growing thin film. In general, the source atoms were introduced approximately 5 Å away from the growing film surface. The initial  $Y$  and  $Z$  coordinates of the incident atom were determined by a random number generator, which was used to generate a common table of 500 initial  $Y$  and  $Z$  coordinates that was utilized for each atom energy. The frequency-of-atom arrival was selected by studying the response of the substrate to the 10-eV atoms. Constant-temperature boundary conditions (CTBC's) and constant-energy boundary conditions (CEBC's) were compared in a simulation of one 10-eV atom striking the atom at the (0, 0, 0) position, the results of which are shown in Fig. 2. With both types of boundary condition the incident atom loses most of its energy within 0.1 ps of being introduced into the system (at  $t=5.011$  ps in this test). Also within this time of 0.1 ps with CTBC the temperature of the substrate plus incident energetic atom had returned to the selected substrate temperature. With CEBC, however, the system continually heats up as energetic particles are added. As a result of this study the CTBC was utilized with a substrate temperature of 300 K, and an atom-arrival frequency of one atom per 0.5 ps. With the CTBC, excess energy in the substrate was dissipated by subtracting a friction force from the atomic forces that was proportional to the product of a damping constant and the excess kinetic energy of the atoms relative to the desired average kinetic energy based upon the desired substrate temperature. Thus the atoms with the highest kinetic energies were damped the most. The relaxation time for the damping force was 0.1 ps. Detailed studies of the histories of individual atom depositions were also performed for initial atom energies of 0.1 and 1 eV, in order to examine the effect of

substrate-atom bonding on the actual impact energies. These calculations were again done with the atom striking the substrate atom at the (0, 0, 0) position. The kinetic energies attained by incoming adatoms immediately before impact were 1.14, 2.27, and 9.92 eV for initial energies of 0.1, 1.0, and 10.0 eV, respectively. Because of the different substrate-atom configurations surrounding different impact points, these arrival energies are expected to vary somewhat during a deposition run. This variation was not examined in detail for reasons of computational efficiency. The effect of the attractive potential on impact energy must be considered, however, in comparing the results for different initial energies.

The arrival rate of 1 atom per 0.5 ps is equivalent to  $1 \times 10^{10}$  monolayers per second, which is much higher than that in any known physical deposition process. At this arrival rate there should be essentially no thermally activated diffusion between arriving atoms as a result of the substrate temperature of 300 K. This is based upon a calculation of the jump frequency to be one per 7 ps for an adatom on a (111) surface, where the activation energy was 0.058 eV and the vibrational frequency was  $1.4 \times 10^{12}$  per second.<sup>20</sup> Thus any significant atom movement between atom arrivals should be as a result of the kinetic energy of the arriving atoms and not due to the substrate temperature. During the full duration of the simulation of 250 ps, some movement of the atoms would occur as a result of the substrate temperature. Since the time scale for this (7 ps) is much larger than the time scale for the arriving atoms (0.5 ps) it would be expected that the contribution from the substrate thermal energy would be the same for all incident-atom energies.

These simulations were conducted on a Cray X-MP/24 super computer. Typical run times for a 500-atom deposition were 20 h of CPU time. During each simulation run, the position and velocities of each substrate and film atom were saved immediately before the release of the next film atom. These large data files were later split and analyzed by a variety of programs to determine atomic redistributions and layer structures. Visualization of the atomic positions was performed with the MACATOMS code of Jones.<sup>21</sup>

## RESULTS

### Surface coverage

The general effect of the energetic atoms can be seen in Figs. 3(a) and 3(b) where the film (light atoms) is shown on the substrate (dark atoms) after the deposition of 200 atoms (1.2 monolayers). Approximately one period of the structure in the film plane is shown for each arrival energy. Figure 3(a) shows that with an incident-atom energy of 0.1 eV the Ag-film atoms form three-dimensional clusters with a significant number of substrate atoms still exposed. Figure 3(b) shows that with 10-eV incident-atom energy the substrate is nearly covered with a monolayer of Ag atoms; most of the additional atoms form a second layer. This interpretation is confirmed by the histograms of the spatial distribution of the atoms in increments of 0.2 Å after the deposition of 200 atoms, as shown in Figs.

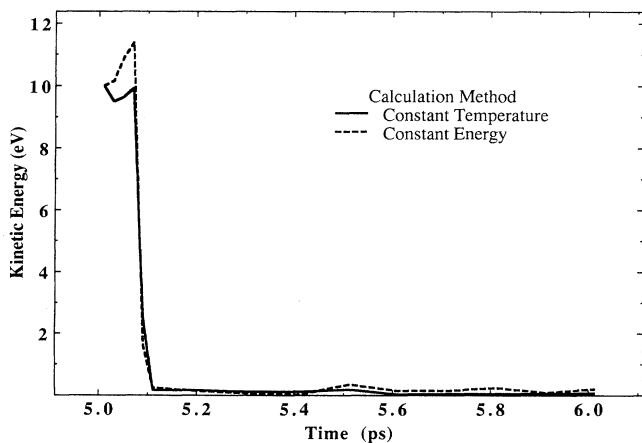


FIG. 2. Comparison of energy loss as a function of time for constant-temperature and constant-energy boundary conditions for a 10-eV particle introduced after 5.011 ps of equilibration at a position 5 Å above the surface and directed at the  $Y=0, Z=0$  position on the surface.

4(a) and 4(b). At the lower incident-atom energies [0.1 eV in Fig. 4(a)] the upper layers of the film fill at the same time as the lower layers but at a smaller rate. Increasing the incident-atom kinetic energy favors growth of the lower layers at the expense of the upper layers. Thus the energetic atoms promote layer-by-layer growth. A kinetic energy of 10 eV per incident atom [Fig. 4(b)] was sufficient to produce essentially a full-monolayer (Frank–Van der Merwe) growth mode. This type of growth continued through the entire 500-atom growth simulation as shown in Figs. 5(a) and 5(b), where histograms similar to those in Fig. 4 are shown after the deposition of 500 atoms (2.98 monolayers). The films made with low atom kinetic energies show a gradual decrease in the numbers of atoms per layer when going away from the substrate-film interface. As the atom kinetic energy is

increased the lower layers fill more completely with few atoms in the upper layers. With 500 atoms deposited at 0.1 eV, however, the lower layers do appear to be filling eventually, as indicated by the near-filled state of the first layer after deposition of approximately three monolayers average coverage.

The progression of the surface coverage with number of atoms deposited was further investigated by determining the occupancy of the first three (111) layers of the film at intervals of 20 deposition steps. This is illustrated in Fig. 6 for the three deposition energies. This view of the process confirms the conclusion that an increase in atom arrival energy promotes layer-by-layer growth. With the exception of the first layer, which obviously begins filling at the same rate as the atom deposition rate for all energies, an increase in arrival energy causes a layer to begin filling at a later stage in the deposition and then to fill more rapidly.

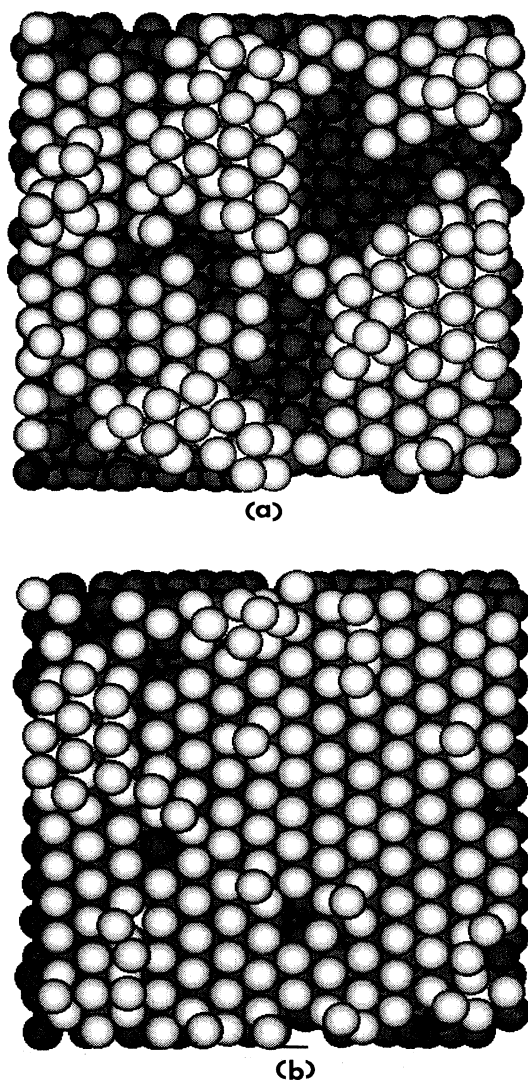


FIG. 3. Atomic configuration after deposition of 200 film atoms (light) onto the substrate (dark atoms) for incident energies of (a) 0.1 eV and (b) 10 eV.

#### Defect incorporation

Aside from unfilled atomic sites, two types of defects were observed in the growing films: stacking faults and

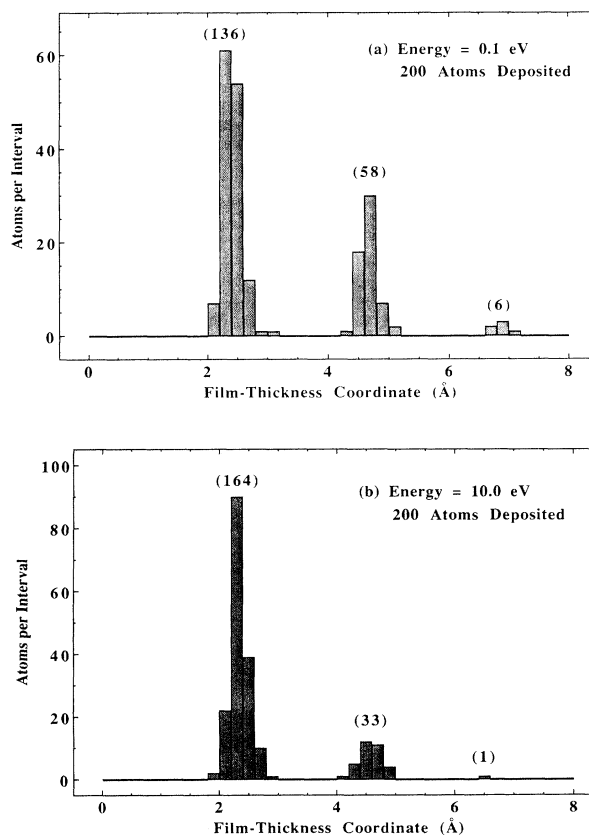


FIG. 4. Histogram of the spatial distribution of atoms in the  $X$  direction for increments of  $0.2 \text{ \AA}$  after the deposition of 200 atoms for energies of (a) 0.1 eV and (b) 10 eV.

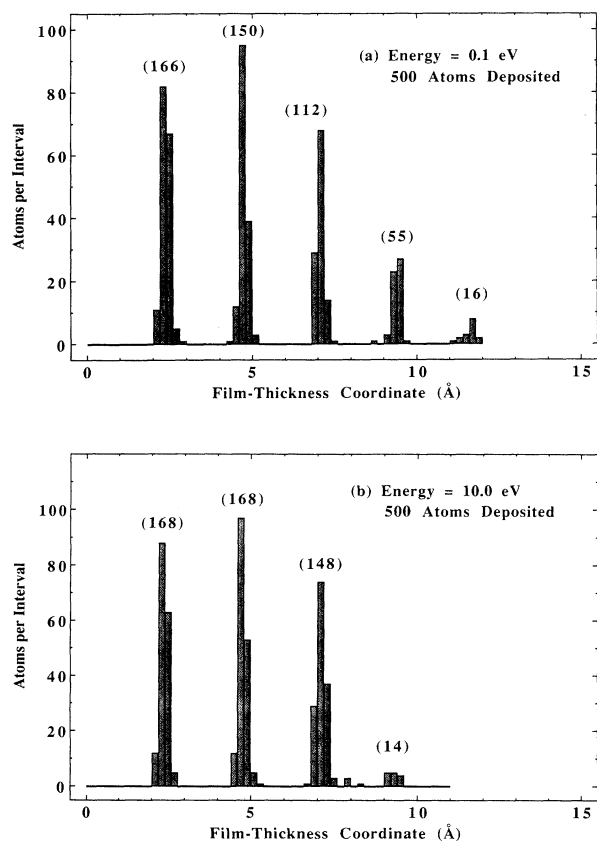


FIG. 5. Histogram of the spatial distribution of atoms in the X direction in increments of  $0.2 \text{ \AA}$  after the deposition of 500 atoms for energies of (a)  $0.1 \text{ eV}$  and (b)  $10.0 \text{ eV}$ .

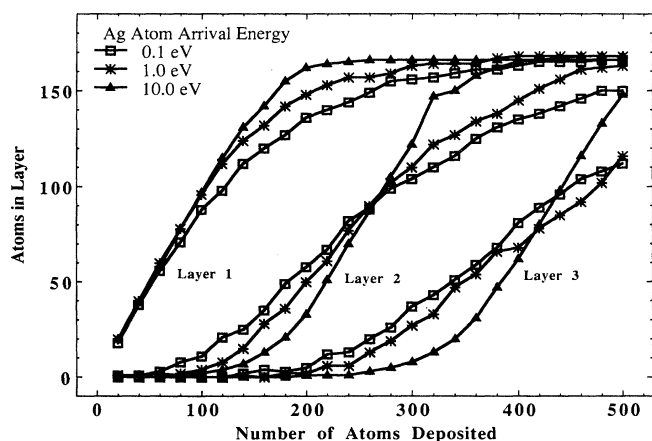


FIG. 6. Number of atoms in the first three layers of the film as a function of the number of atoms deposited for the three incident energies  $0.1$ ,  $1.0$ , and  $10.0 \text{ eV}$ .

partial dislocations separating faulted and unfaulted islands within a layer. For single adatoms and small clusters of adatoms, both perfect-crystal and stacking-fault positions were occupied with approximately equal frequency. This result is consistent with the calculation that the energy of a Ag adatom on a Ag (111) surface is essentially the same in both types of positions.<sup>20</sup> As layers were filled, and islands grew and coalesced, partial dislocations were observed separating faulted and unfaulted islands for all arrival energies. For coverages greater than 70–90%, however, the partial dislocations were observed to annihilate, leaving layers which were each either an all stacking-fault or an all perfect-crystal orientation. The statistics of these calculations were not sufficient to indicate a stacking-fault probability, but after 500 atoms had been deposited, all layers containing more than 160 atoms were of a single orientation, and only layer 1 of the  $0.1\text{-eV}$  film was in a stacking-fault orientation. The observations suggest a prediction of some preference for perfect-crystal stacking, but these calculations give no clear indication of a connection between atom arrival energy and the occurrence of stacking faults. A tendency was seen for the elimination of partial dislocations from nearly filled layers that was most directly connected with the percentage coverage of those layers, rather than atom arrival energy. One must be cautious, however, in interpreting this last result, because the size of the periodic boundaries limited the maximum size of adjacent crystal islands.

None of the atom arrival energies showed any tendency toward forming reentrant cavities of the type reported by Müller for a 2D simulation.<sup>10,11</sup> In all cases where atoms were deposited or displaced into overhanging positions, these configurations were unstable, and the overhanging atom jumped into a layer nearer the substrate. As will be more fully discussed in the section on atomic redistribution mechanisms, this behavior was particularly noticeable for the  $0.1\text{-eV}$  deposition energy, where the collapse of unstable configurations was the major mechanism by which deposited atoms moved in the film.

### Sputtering and mixing

No sputtering of substrate atoms was observed for any of the atom arrival energies. For the  $10\text{-eV}$  arrival energy, however, two previously deposited film atoms were sputtered by the arrival of subsequent particles during the 500-atom deposition run. For the  $0.1$  and  $1.0\text{-eV}$  arrival energies, reflections of one and two atoms, respectively, were observed during the runs. It is interesting that the mechanism of reemission of deposited atoms changed from reflection to sputtering with increasing arrival energy, but the limited statistics did not allow any detailed analysis of the phenomenon.

None of the arrival energies produced any significant mixing between the substrate and the film. Two impacts of film atoms in the  $10\text{-eV}$  run caused substrate atoms to pop out into the first film layer and the deposited atom to embed into the substrate, resulting in two film atoms in the substrate and two substrate atoms in the first film lay-

er. Thus it can be concluded that interface mixing and sputtering of atoms were both very limited at the 10-eV incident-atom energy. The two events that were seen do point to a mechanism by which interface mixing on an atomic scale can occur for particle energies well below those that would cause bulk displacements.

An additional effect on the substrate that occurred only for the 10-eV arrival energy was the movement of substrate atoms from the bottom layer of the substrate onto the lower substrate surface due to directional transmission of energy along chains of atoms. None of these displaced atoms was actually removed from the lower surface. This process, which resulted in ten substrate atoms on the bottom substrate surface after 300 atoms were deposited (no additional effect was observed from this point to the end of the run), is certainly an artifact of the limited thickness of the substrate. It did not, however, significantly disturb the upper substrate surface or its lattice vibrations, and should not have had a significant effect on the calculated film growth. This observation does indicate that no further increase in incident-atom energy would be possible with this size substrate.

#### Atomic transport

In order to distinguish among the several possible mechanisms by which an increased atom arrival energy could promote the layer-by-layer growth of a thin film, a number of different data-reduction schemes were applied to the MDS results. Most of these schemes involved following the motion of film atoms during the deposition run. For this purpose, the motion of film atoms was separated into the motion in the film plane (lateral movement) and the motion normal to the film plane (vertical movement). Both total and stepwise movements were analyzed. In examining the motion between individual deposition steps, a criterion was needed to distinguish between vibrations within an individual lattice site and jumps between sites. For this purpose, a somewhat arbitrary cutoff of 1.5 Å displacement of an atom between deposition steps was chosen as the criterion for an atomic jump. This method may miscount some small jumps, but is much less computationally complex than a determination of site occupancy in a dynamic crystal.

Considering first the lateral motion of the deposited atoms, the average distance moved to the first surface site occupied following deposition showed a definite progression with arrival energy: 0.05 Å at 0.1 eV, 1.5 Å at 1.0 eV, and 2.0 Å at 10 eV. If, however, we look at the average total lateral movement for all 500 atoms from the position where they were deposited to the site they occupy in the film after 500 deposition steps, the trend is less obvious: 3.1 Å at 0.1 eV, 3.0 Å at 1.0 eV, and 4.4 Å at 10 eV. The major effect of increased arrival energy on the total lateral motion was an increased tail in the distribution at large distances, as illustrated in Fig. 7, which compares the lateral motion distributions for 0.1 and 10 eV.

We next considered the vertical motion (perpendicular to the film plane) of atoms after they were initially deposited. For the distributions of total motion between the

step after deposition and the end of the deposition run, the principal trend was a slight *decrease* in the amount of redistribution toward the substrate with increasing energy. This result seemed at first to be contrary to intuition about the process, but is quite sensible once one studies the redistribution mechanisms, as discussed in the following paragraph. A cumulative distribution of the number of vertical redistributions greater than 1.5 Å in each step of the deposition versus the deposition step number revealed different behaviors for the three arrival energies, as shown in Fig. 8. Note that steps both toward and away from the substrate were counted in these distributions. For 1 and 10 eV, the number of jumps begins to increase at about 40 atoms deposited and the 1-eV distribution continues at a steady pace throughout the run. There is a notable increase, however, in the 10-eV data between 140 and 180 atoms deposited (approximately one monolayer coverage) and a smaller increase at 360 atoms deposited. The redistributions of the 0.1-eV atoms do not begin until a much later stage of the deposition, but then proceed at a more rapid rate than that observed for the two higher energies. One must certainly be cautious about assigning steady-state redistribution rates to such a small data sam-

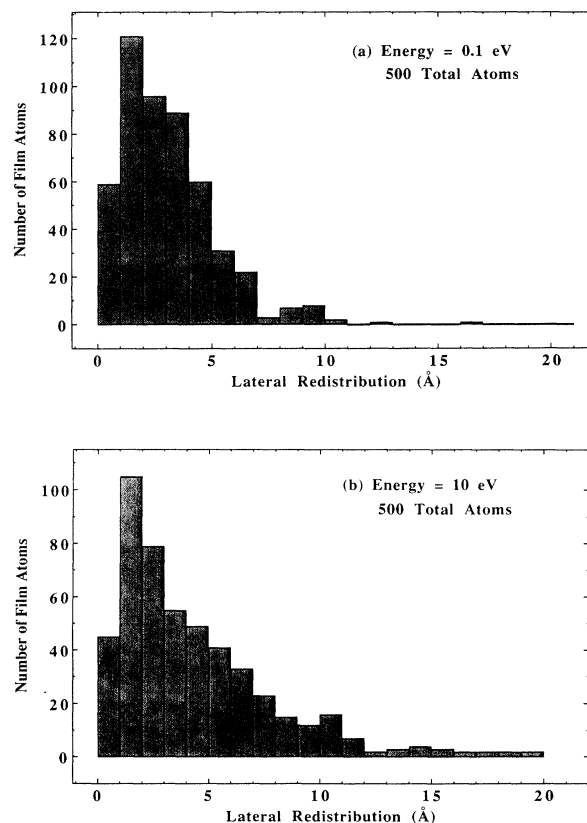


FIG. 7. Histogram of the number of film atoms finally redistributed laterally in increments of 1.0 Å for incident energies of (a) 0.1 eV and (b) 10 eV.

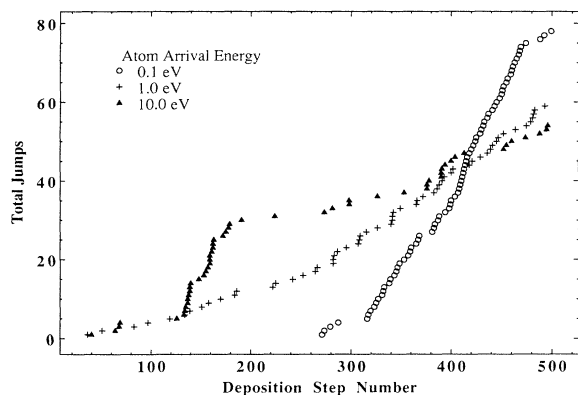


FIG. 8. Cumulative jumps of vertical step size greater than  $1.5 \text{ \AA}$  as a function deposition step number for 0.1-, 1.0-, and 10.0-eV incident energy.

ple, but the average slopes of the cumulative distribution curves do show a decreasing trend with increasing arrival energy (with the exception of the rapid rise of the 10-eV curve near 1 and 2 monolayers).

The vertical redistribution records were used to flag deposition steps that were of interest, and models of these steps were plotted with the MACATOMS code,<sup>21</sup> with the location of the atom deposited in a given step and the initial and final positions of the moving atom separately color coded. Analysis of these images revealed the dominant mechanisms by which the vertical and lateral atomic motions occurred for the three energies. For the 10-eV arrival energy, the atomic movements were almost all caused by the arriving atom directly displacing single film atoms or chains of atoms resulting in the displacement of a film atom into a lower (or sometimes higher) film layer. For some of the events, the deposited atom was embedded in an incomplete film layer. The large number of displacements that occurred between deposition steps 140 and 180 represented a large amount of exchange between the first and second film layers. The fact that the first layer was nearly filled during these steps caused an unusual amount of embedding and ejection of atoms in these steps. The same effect occurred to a much smaller extent when the second film layer was nearly complete. For the 1-eV arrival energy, some atomic movements resulted from the direct displacement phenomenon, except that only single atoms were involved. Approximately an equal amount of atomic movement was caused by the collapse of unstable configurations of overhanging atoms created by the deposition. Often unstable deposited atoms were seen to move to a lower film layer in the step after they were deposited. For the 0.1-eV arrival energy, all of the movement perpendicular to the substrate appeared as the collapse of unstable configurations of overhanging atoms. Many of these collapses occurred in the step after an atom was deposited, implying either that the incoming momentum of the deposited atom was involved or that the activation energy for thermal migration from such sites was extremely low. As noted previ-

ously, no reentrant configurations of the type shown by Müller from his 2D simulations were observed to be stable for longer than a few picoseconds. This change of mechanism from collapse of unstable configurations to direct displacement with increasing arrival energy explains the displacement distributions shown in Fig. 8. At the thermal arrival energy, an atom arriving on a flat layer of the film tends to find a nearby stable location in the layer in which it initially lands. The random arrival positions of atoms result in multilayer islands being formed, producing an atomically rough surface. As this roughness increases, there is an increasing probability that an incoming atom will be deposited on a sloped flank of an island, producing an unstable configuration that causes it to be displaced to a lower film layer. As the deposition energy increases, scattering by and displacement of film atoms in top layers increases, limiting the development of the surface roughness, thereby decreasing the rate at which unstable configurations are produced.

## DISCUSSION

Experimental results indicate that the use of energetic atoms during thin-film deposition promote layer-by-layer growth and that energetic atoms activate surface processes.<sup>4,5</sup> Other than these general observations it is difficult to find any definitive experiments for comparison with our simulation results. This is one of the advantages of a molecular-dynamics simulation; it allows study at an atomic level where experimental observation is still difficult if not impossible. Our full 3D simulations with the realistic EAM should provide a significant improvement in the understanding of the atomic-level process involved in the growth of thin films with energetic atoms.

At low incident-atom energies corresponding to thermal energies the growth mode was by the formation of three-dimensional islands on the surface that subsequently coalesced into a film. Increasing the atom energy to 10 eV changed the three-dimensional islands to a layer-by-layer, or Frank-van der Merwe, growth mode. Previous analytical calculations<sup>22</sup> have shown that the thermal spike following ballistic impact provides insufficient activation to account for the large number of surface-activated processes that were observed in this simulation. Another mechanism that is possible is ballistic impact causing a redistribution of surface atoms; this mechanism was proposed by Müller<sup>10,11</sup> in the form of forward sputtering that filled voids in the growing two-dimensional film.

Our observations are significantly different from those reported by Müller.<sup>10,11</sup> First we observed that severe surface geometries with extensive protrusions and reentrant configurations were naturally unstable in the three-dimensional simulation of deposition on a (111) Ag surface. These types of structures collapsed as a result of the unstable atoms quickly moving to more stable positions in the time steps immediately after deposition. This mechanism was primarily observed at a lower energy of 0.1 eV and to some extent at 1.0 eV. Previous calculations with the EAM indicated that the activation energy for diffusion of a single adatom of Ag on a perfect (111)

Ag surface was only 0.058 eV.<sup>20</sup> The activation energy for atoms in unstable, poorly bonded positions should be even less. For these configurations the activation of the motion could occur by many processes, including normal thermal vibration, the vibration in the thermal spike, or ballistic impact scattering. Unstable configurations of atoms were not present for the 10-eV deposition energy; the film grew on a layer-by-layer basis. For the 10-eV deposition energy, atoms in less stable positions were moved to more stable positions by immediate ballistic impact processes.

From these MDS's there appears to be a driving force to finish a nearly complete atom layer with a minimum of defects. This driving force was observed in two ways. One was the elimination of partial dislocations between islands of different stacking position. The second was the high rate of jumps into layers that was observed when a layer was close to being filled. This was particularly striking in the case of the 10-eV deposition, where steps were observed for the out-of-plane jump rate when layers approached filling.

In the present MDS results the growth was epitaxial for all atom arrival energies, the variable being the topography of the growing surface and the mode-of-film growth. The only lattice defects observed in completed film layers were stacking faults. This calculated epitaxy is not surprising, since it results from the relaxation of deposited atoms into nearby low-energy configurations. The calculations, therefore, tell us little about the effect of energetic particles on epitaxial film deposition. The results, imply, in fact, that elevated temperature or energetic particle impact should not be required for homoepitaxial film growth on the close-packed plane of a fcc metal. This result is consistent with some recent experimental observations. Both homoepitaxial and heteroepitaxial deposition of close-packed metal films at or near room temperature have been reported by a number of authors (e.g., Refs. 23–26). The experimental observations of

room-temperature epitaxy have been made for both thermal<sup>23,24</sup> and energetic<sup>25,26</sup> atom-deposition processes. The critical factors in producing a single-crystal film appear to be a suitable substrate template to promote the desired film orientation and sufficient cleanliness of the deposition to prevent the nucleation of new crystal orientations.

## CONCLUSIONS

(i) Epitaxial growth was observed for all atom energies from 0.1 to 10 eV per atom. This confirms recent experimental observations that in an environment where the surface of a substrate is free of contamination, films will grow in an epitaxial manner even at low substrate temperatures such as 300 K.

(ii) The film topography for 0.1-eV energy incident-silver atoms was in the form of three-dimensional islands.

(iii) The primary mechanism for the redistribution of atoms with 0.1-eV arrival energy was the collapse of unstable clusters.

(iv) The growth changed to layer-by-layer growth or Frank–van der Merwe growth by utilizing incident atoms with 10-eV energy.

(v) A ballistic mechanism was observed for the redistribution of atoms deposited at 10 eV to form complete monolayers.

(vi) Layers with a low density of atoms had atoms in both regular lattice positions and stacking-fault positions with partial dislocations observed separating some of the regions of different stacking. Layers with a high density of atoms were all of one type of stacking with no partial dislocations; layers in both regular and stacking-fault positions with respect to the underlying atoms were observed.

(vii) No cavities or reentrant structures were observed, as had been reported in several MDS's of vapor deposition.

\*Permanent address: School of Engineering and Applied Sciences, The George Washington University, Washington, D.C. 20052.

<sup>1</sup>L. S. Yu, J. M. E. Harper, J. J. Cuomo, and D. A. Smith, *J. Vac. Sci. Technol. A* **4**, 443 (1986).

<sup>2</sup>J. E. Green and S. A. Barnett, *J. Vac. Sci. Technol.* **21**, 235 (1982).

<sup>3</sup>R. D. Bland, G. J. Kominiak, and D. M. Mattox, *J. Vac. Sci. Technol.* **11**, 671 (1974).

<sup>4</sup>C. Schwebel, F. Meyer, G. Gautherin, and C. Pellet, *J. Vac. Sci. Technol. B* **4**, 1153 (1986).

<sup>5</sup>Y. Namba and T. Mori, *J. Vac. Sci. Technol.* **13**, 693 (1976).

<sup>6</sup>D. K. Brice, J. Y. Tsao, and S. T. Picraux, *Nucl. Instrum. Methods B* **44**, 68 (1989).

<sup>7</sup>D. Henderson, M. H. Brodsky, and P. Chaudhari, *Appl. Phys. Lett.* **25**, 641 (1974).

<sup>8</sup>H. J. Leamy, G. H. Gilmer, and A. G. Dirks, in *Current Topics in Materials Science Vol. 6*, edited by E. Kaldis (North-Holland, New York, 1980).

<sup>9</sup>M. Schneider, A. Rahman, and I. K. Schuller, *Phys. Rev. Lett.* **55**, 604 (1985).

<sup>10</sup>K. Müller, *Phys. Rev. B* **35**, 7906 (1987).

<sup>11</sup>K. Müller, *Surf. Sci.* **184**, L375 (1987).

<sup>12</sup>B. W. Dodson, *J. Vac. Sci. Technol. B* **5**, 1393 (1987).

<sup>13</sup>B. W. Dodson and P. A. Taylor, *J. Mater. Rev.* **2**, 805 (1987).

<sup>14</sup>B. W. Dodson, *Phys. Rev. B* **36**, 1068 (1987).

<sup>15</sup>M. S. Daw and M. I. Baskes, *Phys. Rev. B* **29**, 6443 (1984).

<sup>16</sup>S. M. Foiles, M. I. Baskes, and M. S. Daw, *Phys. Rev. B* **33**, 7983 (1986).

<sup>17</sup>M. S. Daw, *Surf. Sci. Lett.* **166**, L161 (1986).

<sup>18</sup>A. Nordsieck, *Math. Comput.* **16**, 22 (1962).

<sup>19</sup>M. S. Daw and S. M. Foiles (unpublished).

<sup>20</sup>W. Rilling, C. M. Gilmore, T. D. Andreadis, and J. A. Sprague, *Can. J. Phys.* **68**, 1035 (1990).

<sup>21</sup>H. D. Jones (unpublished).

<sup>22</sup>C. M. Gilmore, A. Haeri, and J. A. Sprague, *Thin Solid Films* **165**, 359 (1988).

<sup>23</sup>C. A. Chang, *J. Vac. Sci. Technol. A* **8**, 3779 (1990).

<sup>24</sup>R. E. Hummel, A. Morrone, and E. Lambers, *J. Vac. Sci. Technol. A* **8**, 1437 (1990).

<sup>25</sup>I. Yamada, H. Inokawa, and T. Takagi, *J. Appl. Phys.* **56**, 2746 (1984).

<sup>26</sup>P. Bai, G. R. Yang, L. You, T. M. Lu, and D. B. Knorr, *J. Mater. Res.* **5**, 989 (1990).